VIRUS: production of a massively replicated 33k fiber integral field spectrograph for the upgraded Hobby-Eberly Telescope

Hill, Gary, Tuttle, Sarah, Lee, Hanshin, Vattiat, Brian, Cornell, Mark, et al.

Gary J. Hill, Sarah E. Tuttle, Hanshin Lee, Brian L. Vattiat, Mark E. Cornell, D. L. DePoy, Niv Drory, Maximilian H. Fabricius, Andreas Kelz, J. L. Marshall, J. D. Murphy, Travis Prochaska, Richard D. Allen, Ralf Bender, Guillermo Blanc, Taylor Chonis, Gavin Dalton, Karl Gebhardt, John Good, Dionne Haynes, Thomas Jahn, Phillip J. MacQueen, M. D. Rafal, M. M. Roth, R. D. Savage, Jan Snigula, "VIRUS: production of a massively replicated 33k fiber integral field spectrograph for the upgraded Hobby-Eberly Telescope," Proc. SPIE 8446, Ground-based and Airborne Instrumentation for Astronomy IV, 84460N (24 September 2012); doi: 10.1117/12.925434

Event: SPIE Astronomical Telescopes + Instrumentation, 2012, Amsterdam, Netherlands

VIRUS: production of a massively replicated 33k fiber integral field spectrograph for the upgraded Hobby-Eberly Telescope*

Gary. J. Hill[a†], Sarah E. Tuttle[a], Hanshin Lee[a], Brian L. Vattiat[a], Mark E. Cornell[a], D.L. DePoy[c], Niv Drory[d], Maximilian H. Fabricius[e], Andreas Kelz[g,h], J.L. Marshall[c], J. D. Murphy[b], Travis Prochaska[c], Richard D. Allen[c], Ralf Bender[e,f], Guillermo Blanc[i], Taylor Chonis[b], Gavin Dalton[j], Karl Gebhardt[b], John Good[a], Dionne Haynes[g,h], Thomas Jahn[g], Phillip J. MacQueen[a], M.D. Rafal[a], M.M. Roth[g,h], R.D. Savage[a], & Jan Snigula[e]

[a] McDonald Observatory, [b]Department of Astronomy, University of Texas at Austin, 1 University Station, Austin, TX 78712-0259, USA

[c] Department of Physics and Astronomy, Texas A&M University, 4242 TAMU, College Station, TX 77843-4242, USA

[d] Instituto de Astronomía, Universidad Nacional Autónoma de México, Avenida Universidad 3000, C.P. 04510, D.F., México

[e] Max-Planck-Institut für Extraterrestriche-Physik, Giessenbachstrasse, D-85748 Garching b. München, Germany

[f] Universitäts-Sternwarte München, Scheinerstr. 1 , 81679 München, Germany

[g] Leibniz Institute for Astrophysics, An der Sternwarte 16, 14482 Potsdam, Germany

[h] innoFSPEC Potsdam, An der Sternwarte 16, 14482 Potsdam, Germany

[i] Observatories of the Carnegie Institution for Science, 813 Santa Barbara Street, Pasadena, CA 91101, USA

[i] Department of Physics, Oxford University, Denys Wilkinson Building, Keble Road, Oxford, OX1 3RH, UK

ABSTRACT

The Visible Integral-field Replicable Unit Spectrograph (VIRUS) consists of a baseline build of 150 identical spectrographs (arrayed as 75 units, each with a pair of spectrographs) fed by 33,600 fibers, each 1.5 arcsec diameter, deployed over the 22 arcminute field of the upgraded 10 m Hobby-Eberly Telescope (HET). The goal is to deploy 82 units. VIRUS has a fixed bandpass of 350-550 nm and resolving power R~700. VIRUS is the first example of industrial-scale replication applied to optical astronomy and is capable of spectral surveys of large areas of sky. This approach, in which a relatively simple, inexpensive, unit spectrograph is copied in large numbers, offers significant savings of engineering effort, cost, and schedule when compared to traditional instruments.

The main motivator for VIRUS is to map the evolution of dark energy for the Hobby-Eberly Telescope Dark Energy Experiment (HETDEX‡) using 0.8M Lyman-α emitting galaxies as tracers. The full VIRUS array is due to be deployed by early 2014 and will provide a powerful new facility instrument for the HET, well suited to the survey niche of the telescope. VIRUS and HET will open up wide-field surveys of the emission-line universe for the first time. We present the production design and current status of VIRUS.

---

* The Hobby – Eberly Telescope is operated by McDonald Observatory on behalf of the University of Texas at Austin, Pennsylvania State University, Ludwig-Maximillians-Universität München, and Georg-August-Universität, Göttingen

† G.J.H.: E-mail: hill@astro.as.utexas.edu

‡ http://hetdex.org/

Ground-based and Airborne Instrumentation for Astronomy IV, edited by Ian S. McLean, Suzanne K. Ramsay, Hideki Takami, Proc. of SPIE Vol. 8446, 84460N · © 2012 SPIE · CCC code: 0277-786X/12/$18 · doi: 10.1117/12.925434

Keywords: Telescopes: Hobby-Eberly, Astronomical instrumentation: Spectrographs, Spectrographs: VIRUS, Spectrographs: Integral Field, Spectrographs: performance

1. INTRODUCTION: HET WIDE FIELD UPGRADE AND INDUSTRIAL REPLICATION OF VIRUS

Large, targeted, spectroscopic surveys of continuum-selected objects are now becoming the norm, and have greatly increased our understanding in many areas of astronomy. Surveys of the emission-line universe, however, are limited currently to wide field imaging with narrow band filters[1], or to narrower fields with Fabry-Perot etalons or adaptations of imaging spectrographs[2]. Integral field (IF) spectrographs offer a huge gain over these techniques, depending on the application, providing greater sensitivity and wavelength coverage as well as true spectroscopy. The current generation of IF spectrographs is well-adapted to arcminute-scale fields of view, with several thousand spatial elements, and adequate spectral coverage for targeted observations of individual extended objects. They have the grasp to detect simultaneously of order 0.5 million (spectral x spatial) resolution elements.

In order to undertake large-scale surveys for emission-line objects, much greater field coverage is needed. Narrow-band imaging surveys can now cover large areas, but often require spectroscopic follow-up, and still do not probe sufficient volume to detect rare objects or to overcome cosmic variance. Wide-field IF spectroscopy is hard to achieve without a large multiplexing factor, so we have embarked on a program to produce an instrument that uses large-scale replication to create a unique astronomical facility capable of spectroscopic surveys of hundreds of square degrees of sky. The instrument is the Visible Integral-field Replicable Unit Spectrograph (VIRUS)[3-5], a simple, modular integral field spectrograph that is to be replicated at least 150-fold, to provide an order of magnitude increase in grasp over any existing spectrograph, when mounted on the upgraded Hobby-Eberly Telescope (HET)[6-8]. Fig. 1 shows the upgraded HET as it will appear in approximately 18 months from now.

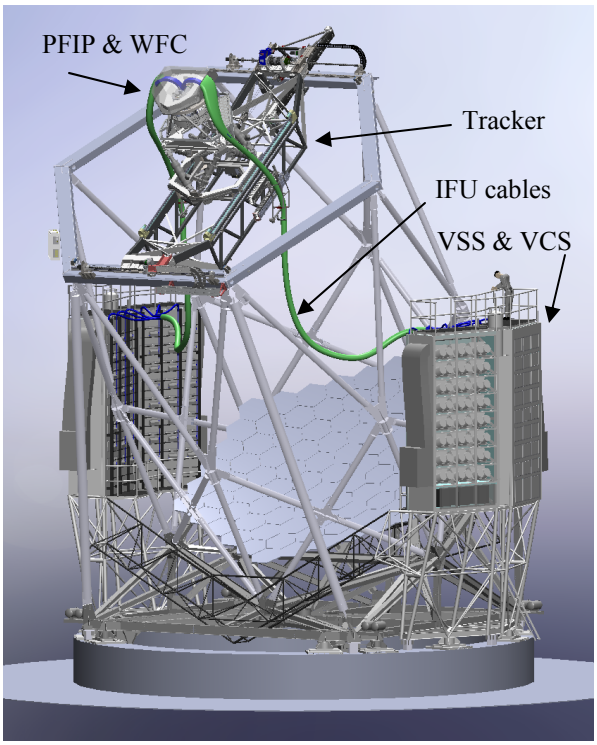

Figure 1 – Upgraded HET as it will appear in late 2013. The new tracker supports the Wide Field Corrector (WFC) and Prime Focus Instrument Package (PFIP). The fiber cables run about 20 m to the four enclosures of the VIRUS Support Structure and Cryogenic System (VSS & VCS) that houses the 75 to 82 pairs of integral field spectrographs that make up VIRUS.

The traditional astronomical instrument has a monolithic design and is a one-off prototype, where a large fraction of the cost is expended on engineering effort. When compared to monolithic instruments, there are cost savings from creating several copies of a spectrograph to gain multiplex advantage, because the components are less expensive and the engineering is amortized over the production run. As an example, the new MUSE[9] instrument for ESO VLT will field-slice a 1 arcmin. square field into 24 duplicated spectrographs. VIRUS makes the next step, and exploits industrial-scale replication, which we (arbitrarily) define to be in excess of 100 spectrograph channels. We build upon the concepts laid out in Refs. 3-5, where we concluded that industrial replication offers significant cost-advantages when compared to a traditional monolithic spectrograph, particularly in the cost of the optics and engineering effort. This concept breaks new ground in optical instruments, and appears to be a cost-effective approach to outfitting the coming generation of ELTs, for certain instrument types, where the multiplex advantage of an integral field can avoid growth in the scale of instruments with telescope aperture.

The motivation for VIRUS is the Hobby-Eberly Telescope Dark Energy Experiment (HETDEX[10-11]), which will map the spatial distribution of about 0.8 million Lyα emitting galaxies (LAEs) with redshifts $1.9 < z < 3.5$ over a 420 sq. deg. area (9 Gpc^3) in the north Galactic cap, using VIRUS on the upgraded HET. This dataset will constrain the expansion history of the Universe to 1% and provide significant constraints on the

evolution of dark energy. The advantage of an IF spectrograph for this project is that the tracer galaxies are identified and have their redshifts determined in one observation.

Each VIRUS unit is fed by 224 fibers that each cover 1.8 arcsec^2 on the sky. The fibers feeding a two-unit module are arrayed in a 50×50 arcsec^2 IFU with a 1/3 fill-factor. A dither pattern of three exposures fills in the area. The spectral resolution is 0.57 nm, with coverage of 350–550 nm. The optical design is simple, using three reflective and two refractive elements. With dielectric reflective coatings optimized for the wavelength range, high throughput is obtained. The full VIRUS array will simultaneously observe a minimum of 33,600 spectra with 12 million resolution elements. The IFUs are arrayed within the 22′ field of the upgraded HET with ~1/4.5 fill factor, sufficient to detect the required density of LAEs for HETDEX. Development started with the prototype Mitchell Spectrograph (formerly VIRUS-P[4]), deployed in October 2006, and the production prototype where value engineering were used to reduce the cost for production. VIRUS is now in production, and we present here the design and lessons learned in moving from prototype to production.

The HET[12-15] is the prototype of a new breed of cost-effective large telescopes, and is the basis for the Southern African Large Telescope (SALT)[16]. HET is an innovative telescope with an 11 m hexagonal-shaped spherical mirror made of 91 1-m hexagonal segments that sits at a fixed zenith angle of 35^o. It can be moved in azimuth to access about 70% of the sky visible at McDonald Observatory (δ = -10.3^o to +71.6^o). The pupil is 9.2 m in diameter, and sweeps over the primary mirror as the x-y tracker follows objects for between 50 minutes (in the south at δ = -10.0^o) and 2.8 hours (in the north at δ = +67.2^o). The maximum time on target per night is 5 hours and occurs at +63^o. The HET primary mirror has a radius of curvature of 26164 mm, and the current 4-mirror double-Gregorian type corrector is designed to produce images with FWHM < 0.6 arcsec in the absence of seeing, over a 4 arcmin (50 mm) diameter science field of view. Detailed descriptions of the HET and its commissioning can be found in refs 12-15.

The HET was originally envisioned as a spectroscopic survey telescope, able to efficiently survey objects over wide areas of sky. While the telescope has been very successful at observing large samples of objects such as QSOs spread over the sky with surface densities of around one per 10 sq. degrees, the HET design coupled with the limited field of view of the corrector hampers programs where objects have higher sky densities. In seeking a strong niche for the HET going forward, we desire a wide field of view coupled with a highly multiplexed spectrograph in order to exploit the strengths of the telescope and of the site.

The requirement to survey large areas of sky with VIRUS plus the need to acquire wavefront sensing stars to provide full feedback on the tracker position led us to design an ambitious new corrector employing meter-scale aspheric mirrors and covering a 22-arcmin diameter field of view. The HET Wide Field Upgrade (WFU) deploys the wide field corrector (WFC[17]), a new tracker prime focus instrument package (PFIP), and new metrology systems[6-8]. The new corrector has improved image quality and a 10 m pupil diameter. The periphery of the field will be used for guiding and wavefront sensing to provide the necessary feedback to keep the telescope correctly aligned. The WFC will give 30 times larger observing area than the current HET corrector. It is a four-mirror design with two concave 1 meter diameter mirrors, one concave 0.9 meter diameter mirror, and one convex 0.23 m diameter mirror. The corrector is designed for feeding optical fibers at f/3.65 to minimize focal ratio degradation, and so the chief ray from all field angles is normal to the focal surface. This is achieved with a concave spherical focal surface centered on the exit pupil. The primary mirror spherical aberration and the off-axis aberrations in the wide field are controllable due to the first two mirrors being near pupils, and the second two mirrors being well separated from pupils. The imaging performance is 0.6 arcsec or better over the entire field of view, and vignetting is minimal. The WFC is being manufactured by the University of Arizona College of Optical Sciences. Delivery is projected for Q2 2013.

A new tracker is needed to accommodate the size and five-fold weight increase of the new PFIP. It will be a third generation evolution of the trackers for HET and SALT, and is in essence a precision six-axis stage. The tracker is being developed by the Center for Electro-Mechanics (CEM) at the University of Texas at Austin[18-27], with integration complete at the CEM facility, and testing about to begin.

HET requires constant monitoring and updating of the position of its components in order to deliver good images. The WFC must be positioned to 10 μm precision in focus and X,Y, and 4.0 arcsec in tip/tilt with respect to the optical axis of the primary mirror. This axis changes constantly as the telescope tracks, following the sidereal motions of the stars. Tilts of the WFC cause comatic images. In addition, the global radius of curvature of the primary mirror can change with temperature (as it is essentially a glass veneer on a steel truss), and needs to be monitored. The segment alignment maintenance system (SAMS) maintains the positions of the 91 mirrors with respect to each other, but is less

sensitive to the global radius of curvature of the surface. The feedback to maintain these alignments requires excellent metrology, which is provided by the following subsystems:

- Guide probes to monitor the position on the sky, and plate scale of the optical system, and monitor the image quality and atmospheric transparency
- Wavefront sensors (WFS) to monitor the focus and tilt of the WFC
- Distance measuring interferometer (DMI) to maintain the physical distance between the WFC and primary mirror
- Tip-tilt sensor (TTS) to monitor the tip/tilt of the WFC with respect to the optical axis of the primary mirror

The upgrade adds wavefront sensing [7,8,28-32] to HET in order to close the control loop on all axes of the system, in conjunction with the DMI and TTS adapted from the current tracker metrology system. There is redundancy built into the new metrology system in order to obtain the highest reliability. Two guide probes distributed around the periphery of the field of view provide feedback on position, rotation, and plate scale, as well as providing a record of image quality and transparency. The alignment of the corrector is monitored by the wavefront sensors as well as by the DMI and TTS. The radius of curvature of the primary mirror is monitored by the combination of focus position from the WFS with the physical measurement from the DMI and checked by the plate scale measured from the positions of guide stars on the guide probes. The SAMS edge-sensors provide a less sensitive but redundant feedback on radius of curvature as well.

Two guide probes will use small pick-off mirrors and coherent imaging fiber bundles to select guide stars from the outer annulus of the field of view. They will be located ahead of the focal surface, before the shutter. Each will range around the focal surface on precision encoded stages, accessing a 180 degree sector. They are designed to have a small size to reduce shadowing of the focal surface, and each will have a field of view of 22.6 arcsec on a side. During setup on a new target, they will be driven to pre-defined positions, and the initial pointing will be made by centering the guide stars in the probes. This system is a significant upgrade from the current pellicle-based guiders.

Two Shack-Hartmann (S-H) wavefront sensors will also range in the outer field. Their function is to provide feedback on the low-order errors in the wavefront (focus, coma, spherical, and astigmatism)[28-31]. These errors are caused by misalignment of the corrector with the primary mirror focal surface and by global radius of curvature and astigmatism errors in the primary mirror shape. Updates will be generated approximately once per minute. In addition to the WFS probes there will be an analysis wavefront sensor as part of the acquisition camera that will allow more detailed feedback analysis of the image quality, simultaneous with the operation of the WFS probes, independent of seeing. Simulations show that a S-H system with 7x7 sub-apertures across the pupil can meet the requirements using 18th magnitude stars. We have deployed a wavefront sensor for the current HET with 19 sub-apertures across the pupil and the final design is being informed by direct experience with this sensor. The design of the wavefront sensors is straightforward, but their application to the HET, with the varying illumination of the telescope pupil during a track, requires development of a robust software system for analysis of the sensor data to produce reliable wavefront information[30].

2. VIRUS SCIENCE REQUIREMENTS

The design of VIRUS flows directly from the requirements for HETDEX[10,11], to maximize the number of LAEs detected in a set observing time, and to span sufficient redshift range to survey the required volume. These science requirements flow down to the following technical requirements for VIRUS:

- Coverage of $\Delta z \sim 2$ and coverage into the ultraviolet to detect LAEs at the lowest possible redshift. VIRUS is designed for $350 < \lambda < 550$ nm or $1.9 < z < 3.5$
- Resolution matching the linewidth of LAEs (R~700) to maximize detectability.
- Minimum throughput on sky (including atmosphere) ranging between 5% at 350 nm, 15% at 450 nm, and 10% at 550 nm to reach sensitivity of 3-4x10^{-17} erg/cm^2/s in 20 minutes on HET.
- Low read noise detector (~3 electrons) to achieve sky-background dominated observations in 360 seconds
- High stability to ambient temperature variations, though not to gravity variations since the VIRUS modules will be fixed on HET.
- Simple, inexpensive design.

These principles guided the development of VIRUS and the prototype, as described in Sections 3 and 4.

3. THE VIRUS PROTOTYPE: MITCHELL SPECTROGRAPH (VIRUS-P)

The motivation for building the VIRUS prototype (Mitchell Spectrograph, formerly VIRUS-P[4]) was to provide an end-to-end test of the concepts behind HETDEX, both instrumental and scientific. Construction and testing of the prototype have verified the opto-mechanical design, the throughput, the sensitivity, and demonstrated the utility of such an instrument for surveys of emission-line objects. It has also served as a test-bed for the software development needed for analyzing the data from the full VIRUS array. The parallel nature of VIRUS means that the prototype can be used to develop the final software pipeline. The Mitchell Spectrograph was also designed to be a facility instrument on the McDonald 2.7 m Smith Reflector. On the 2.7 m at f/3.65, the 200 μm fiber cores subtend 4.1 arcsec, and the IFU covers 3.5 arcmin^2. While the fibers are large, projected on the sky, the IFU covers the largest area of any current IF spectrograph and this results in great sensitivity for wide area surveys and particularly for spatially extended low surface brightness emission[33]. Other science applications have included high redshift radio galaxies[34], and studies of resolved nearby galaxies[35-37]

The Mitchell Spectrograph has been used for a pilot survey of Ly-α emitting galaxies in support of the HETDEX project (HPS, Refs 38-40). The survey covers 166.4 arcmin^2 on the COSMOS, MUNICS-S2, and GOODS-N fields and detects 107 LAEs and 368 low redshift emitters[38]. The results of the HPS confirm the sensitivity estimates on which HETDEX is based[39], and demonstrate the effectiveness of blind IFU spectroscopy for this application. The HPS sample is unique in the volume it probes, when compared to narrow band searches which reach deeper but are highly influenced by cosmic variance, and includes a significant number of luminous LAEs which have allowed follow up in the near infrared to study rest-frame optical emission lines of H-a, H-b, and [OIII] yielding interesting results on the metallicities of these objects[40].

The VIRUS instrument consists of three basic sub-units: the IFU, the collimator/grating assembly, and the camera assembly. The beam size is 125 mm, allowing the collimator to accept an f/3.32 beam from the fibers, accommodating a small amount of focal ratio degradation of the f/3.65 input from the telescope. The camera is a f/1.33 vacuum Schmidt design with a 2k x 2k @ 15 μm pixel CCD at its internal focus.

Detailed discussion of the performance of the Mitchell Spectrograph is presented in Ref. 4, here we summarize the results:

- Throughput of the Mitchell Spectrograph as a function of wavelength (ignoring aperture effects at the input to the fibers) peaks at 40% with 15 m long fibers, in line with predictions based on the measured throughputs of individual components. On-sky at the HJST, including the atmosphere, the throughput peaks at 18%. This performance meets or exceeds that required for HETDEX, when projected HET throughput is considered, except at the very shortest wavelengths.
- The 5-σ point source line flux sensitivity is ~5x10^{-17} erg/cm^2/s, in 2 hours observing, in line with predictions. The number of emission-line galaxies detected in the HPS are in line with predictions, confirming the models on which HETDEX predictions are based.
- Image quality of the instrument meets requirements. Optical alignment was achieved with simple setup procedures.
- The instrument is extremely stable against temperature changes, with images moving 1/20 of a resolution element with a 12 Celsius temperature change, exceeding requirements. On HET, the VIRUS units will be mounted fixed, so stability against gravity vector changes is not a requirement.

4. VIRUS PRODUCTION DESIGN

Evolution of the design of VIRUS from the prototype to the production model was made in two steps. First a pre-production prototype was developed that incorporates the production engineering to reduce costs. In particular aluminum and Invar castings for components including the cryostat were prototyped and qualified. Second, small design modifications gleaned from this experience have been incorporated into the First Article production unit and we are now in production with an initial batch of 8 units, followed by full production later this year.

VIRUS naturally splits into three major subsystems (IFU, collimator, and camera), which have kinematic interfaces between them. The opto-mechanical tolerances have been allocated so as to allow the interchangeability of the IFUs and

cameras on collimators without the need for any realignment, as described in Ref. 41. This interchangeability allows the subunits to be assembled, aligned, and tested in separate places and to then be integrated at the HET. Cameras are being produced at UT Austin, collimators at TAMU, and IFUs at AIP. Oxford University is providing a large number of mechanical parts for the collimators and cameras.

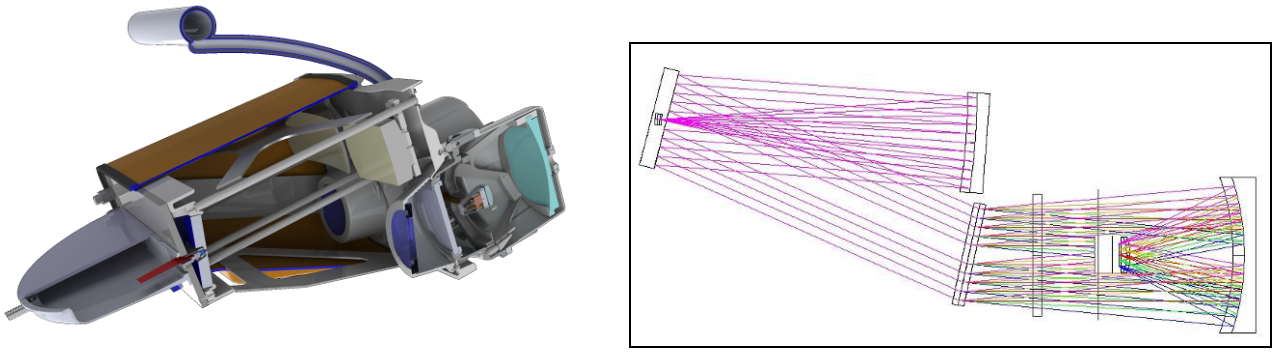

Figure 2: Layout of the production VIRUS. Left shows the production mechanical design and right shows the optical design. The grating has 930 l/mm and the coverage is fixed at 350-550 nm. The mechanical cutaway shows the IFU slit assembly on the left, mounted to the collimator. The Schmidt camera has an internal CCD in the vacuum and mounts to the main bulkhead of the collimator. It is cooled by a flexible line from above with a breakable cryogenic bayonet connection.

4.1 VIRUS Production Optomechanical Design

While the VIRUS units are mounted in fixed housings, their enclosures track ambient temperature and they are required to operate with high stability under a wide range of temperature from -5 to +25 degrees Celsius. The instrument is specified to not require recalibrating for shifts in the positions of the fiber spectra over the temperature range encountered in an hour, with the goal of maintaining alignment during an entire night. Stability is crucial since the data analysis is sensitive to 0.1 pixel shifts in the spectra. This requirement corresponds to shifts smaller than 0.5 pixels (1/10 of a resolution element) at the detector for 5 degrees Celsius temperature change. The Mitchell Spectrograph was designed to test this requirement. It is mounted in a gimbal to maintain its orientation, but sees the full temperature swing in a night.

For production, we made some significant changes to the design, based on experience with the Mitchell Spectrograph and responding to the development for the HET WFU design. The most significant was to double the spectrographs so that a pair shares a single IFU, a common collimator housing, and a common cryostat (Fig. 2). The motivation for this came first from fiber cable handling: it is more efficient in terms of weight and cross-sectional area to double the number of fibers in a cable (note that the fiber itself is not the dominant weight in a bundle). There is not a significant cost-savings on the IFU, since the majority of the cost is in the fiber, but volume occupied by the cables is reduced and the cable handling becomes significantly easier with 75 instead of 150 cables to accommodate (the goal is 82 cables, and the IFU handling system is being designed with enough capacity for 92). The other advantage to the double unit is that two cameras share a vacuum, and have a single connection to the LN_2 cooling system. This increases the volume in an individual cryostat, which increases hold-time, and saves cost on vacuum valves and other fixturing. Pairing the spectrographs enabled reduction of mechanical structure to support optics by eliminating the redundant structure of two spectrographs placed side-by-side. The complexity of the enclosures to house the spectrographs was also be reduced by pairing the instruments because fewer interfacial features between instrument and superstructure are required.

The optical layout has been modified to make the system more linear and allow the units to be packed more tightly in the housings (Fig. 2). Analysis of the fiber diameter for maximizing the number of Lyman-α emitting (LAE) galaxies detected by the HETDEX survey indicates that the ideal is 1.5 arcsec for the expected range of image quality to be encountered in the survey (1.3 to 1.8 arcsec FWHM). Analysis of the expected number of LAEs with redshift also indicates that the majority of the objects are located at $z<3.5$ due to the change in distance modulus with redshift coupled with the steepness of the LAE luminosity function. As a result, the decision has been made to reduce the wavelength coverage so as to preserve spectral resolution, while accommodating the larger fibers (266 vs 200 μm core diameter). This is a small change and the increase in dispersion of the grating (930 versus 830 l/mm used for the HPS)

does not effect diffraction efficiency over the observed bandpass. Wavelength coverage is 350 – 550 nm ($1.9 < z < 3.5$) and resolving power is R=700 at 450 nm. Fig. 3 shows an exploded view of the spectrograph unit.

The VIRUS optics and mechanical interfaces have been carefully specified to produce optics that will be interchangeable amongst any VIRUS unit. Both the optical and mechanical properties of each optic have been carefully toleranced using Monte Carlo realizations of the collimator and camera that were then combined and evaluated. The optical tolerancing is described in detail in Ref 41. Particular attention was paid to the relative alignment of the axes of the two spectrographs within a single unit. Analysis predicts that any camera can be used with any collimator, and will enable quick assembly of the optical assemblies and spectrograph units. This will be tested shortly with the first production batch.

Detailed information on the VIRUS mechanical design is given in Refs 42-44. Relatively early in the production mechanical design of VIRUS we investigated castings for large aluminum bulkhead parts. Castings offer the potential to produce part shapes which might otherwise be impossible or prohibitively expensive to machine from a solid billet of material. As a result they offer the designer structures that are exceedingly lightweight and stiff. Casting is often characterized by its lack of precision and repeatability which does not lend itself well to producing instrumentation. In addition, casting processes traditionally require high up-front costs for fabricating the molds making them uneconomical for low-quantity production and risky for design efforts where prototyping is required. We have adapted our design to these factors, and the recent proliferation of stereo lithography and other rapid prototyping devices has significantly decreased the cost of producing prototype castings. Complex part shapes are quickly and economically "printed" using stereo lithography equipment or machined from plastic foam. Those parts can then be used to imprint sand molds or in the case of investment casting, coated with refractory material and melted out through a sprue. Several companies offer fast turnaround, low cost prototype casting services and can accept CAD models online without need for mechanical drawings. As a result, we were able to prototype subassemblies with castings without incurring prohibitive costs, and were able to gain an understanding of the design principles needed in using castings.

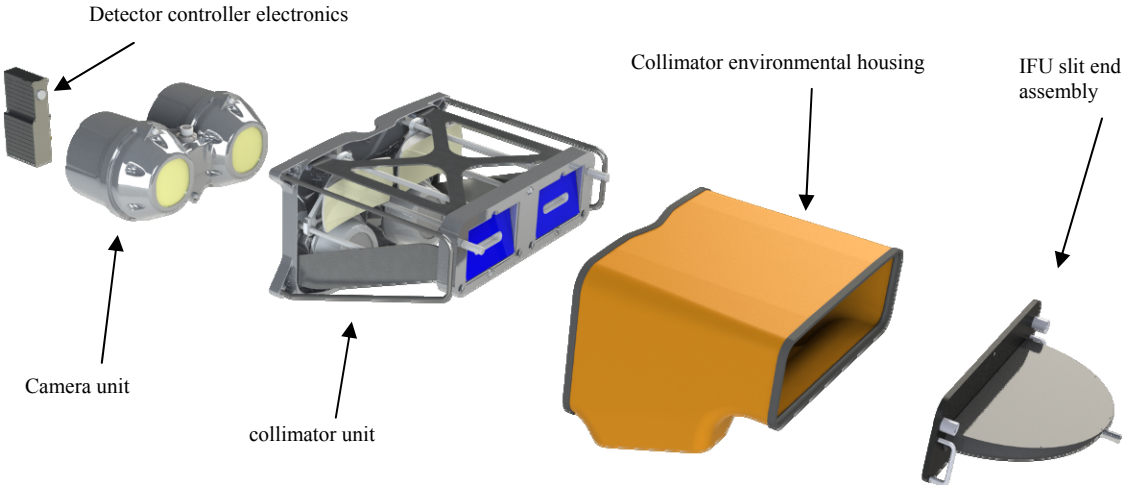

Figure 3. Basic components of the VIRUS unit housing two spectrographs. Light enters at the IFU slit assembly along two axes. The collimator holds the IFU and camera cryostat on kinematic mounts and forms the main structure of the instrument. The cameras are interchangeable and removable should maintenance be required. The detector controllers mount directly to the cryostats.

In the final design, we adopted cast aluminum cryostats and cast Invar detector supports. Prototyping of aluminum castings for the major bulkheads in the collimator demonstrated that the part-to-part variation (due primarily to warping of the cast parts) required significant labor in setting the parts up for post-machining. We were able to prove the concept and produced collimator structures within specification, but in the end we adopted bulkheads machined from large billets of aluminum jig stock. This represented the cheaper alternative for the Oxford Physics machine shop due to high labor costs coupled with large CNC mill capacity. They have adopted a production sequence that involves very low labor to set up and machine each bulkhead.

Kinematic mounts enable highly repeatable registration between components and their use is prevalent in precision optical assemblies. The VIRUS spectrograph relies on kinematic mounts between sub-assemblies which are considered modular to each other, specifically the IFU slit assembly, the collimator, and the camera. The optical and mechanical tolerances of the instrument are arranged such that modules of a particular type would be interchangeable. For example, the camera couples to the collimator through a kinematic mount. It is required that any camera could be used with any collimator and perform within specification. Similarly, the VPH gratings are modular to the collimator and the detector sub-assemblies are modular to the camera body.

4.2 Gratings

VIRUS uses volume phase holographic (VPH) gratings, which offer high efficiency and low cost. The setup for HETDEX employs VPH gratings with physical dimensions of 148 mm in diameter by 16 mm in total thickness; the VPH layer itself has a 138 mm diameter clear aperture and is sandwiched between two 8 mm thick, anti-reflection (AR) coated fused silica substrates using an optical grade adhesive. The grating has a fringe frequency of 930 lines/mm and operates at order m = 1 in transmission from 350 to 550 nm for unpolarized light. Efficiency is optimized for the UV by lowering the angle of incidence from the Bragg angle which is close to 12 degrees.

Details of the grating design and testing are reported in Refs. 47,48. We have undertaken tests of small and full size gratings from Wasatch Photonics, Kaiser Optical Systems International (KOSI), and SyZyGy using a custom automated test-bench that can fully characterize a grating over a range of input and output angles. This test bench has been used to evaluate test gratings as it allows orders m=-1,0,1,2 to be measured to account for as much of the diffracted light as possible[48]. Performance in the ultraviolet has been enhanced by reducing the angle of incidence to shift the blaze to the UV. Angle changes of the grating at fixed collimator angle have little effect on the wavelength range, so tilting the grating provides an independent free parameter in tuning the throughput as a function of wavelength. In addition we have specified a 1 deg. tilt of the fringes in the grating, to ensure that the "Litterow" Ghost[49] is off the detector for the VIRUS configuration.

In order to ensure a standardized reference for measurements of diffraction efficiency of production gratings compared to specifications, and to facilitate more rapid testing than possible with the flexible test bench mentioned above, we have developed a simple rugged grating tester for the specific gratings we are procuring for VIRUS[48]. LEDs with wavelengths of 350,450, and 550 nm illuminate 12.5 mm subaperture on the grating surface. The angles of incidence and diffraction are fixed to the VIRUS configuration and the light is imaged onto a 2/3 format commercial CCD camera by an off-the-shelf aspheric lens. The position of the grating can be moved laterally to sample 9 subapertures in order to provide an average efficiency more representative than spot measurements. We have found that VPH gratings exhibit quite significant small-scale variations in efficiency and it is possible to find a "hot-spot" in the diffraction efficiency, if too small an area is measured. This is particularly the case with laser measurements employed by some vendors. The grating tester is tailored to the properties we care about in the specification and avoids conflicts over inconsistent measurement methods. At the time of writing the grating contract is about to be awarded, with production expected to spread over 12 months.

4.3 Camera and Detector System

The camera cryostat vacuum is shared between a pair of spectrographs. This modification effectively halves the number of ancillary vacuum components such as valves and vacuum gauges. This saves not only the expense of these components but reduces the number of sealing surfaces which contribute to long-term vacuum degradation and are a point of failure. The larger evacuated volume also leads to longer vacuum hold-time. Similarly, the cryogenic cooling system is shared within a unit. This reduces the part count of the instrument cryogenic system and also simplifies the cryogenic distribution system and losses associated with fittings and valves. The cryogenic system development and testing is described in greater detail in Sec. 5.1 and Ref. 50. The cryostat is composed of two aluminum castings, post-machined on critical mount surfaces and flanges. Cryostats are being manufactured by MKS Inc., and have been evaluated extensively. An impregnating step with Locktite Resinol, following machining, ensures that the porosity of the cast aluminum does not lead to virtual leaks or poor vacuum seals, and leak rates are achieved that are consistent with the O-ring length and internal volume of the cryostat. While the tooling cost for casting is quite significant, the cost for even a single cryostat of this size is competitive with machining from bulk stock, and is much cheaper for for the VIRUS production run. Cryostats are being delivered at a rate of 5 per week. Production is discussed in Ref. 44.

The stability of the instrument to temperature changes is crucial, as discussed above. While the Mitchell Spectrograph design was very successful in this regard, we have traced the small instability with ambient temperature swings to movement of the camera mirror. In VIRUS the detector head assembly is all Invar with a cast "spider" mounting the detector and field flattener and an Invar truss structure supporting the mirror (Figs. 4,5).

The CCDs for VIRUS have 2kx2k format with 15 μm pixels. The required readout time is relatively slow at 20 seconds, binned 2x1, but low read noise (~3 electrons) is required and the parallel readout of up to 164 CCDs is still challenging. The data volume from the full VIRUS array is about 2.5 GB per observation. Observation times per field are 20 minutes for the HETDEX survey, split into three exposures, and we expect to generate 40 TB of raw data over the course of the survey, including calibrations. These data volumes are quite modest in the context of the coming generation of large imaging surveys, even though the VIRUS CCD system at 0.7 Gpxl is similar in size to the latest generation of wide field imagers. The data reduction pipeline Cure[51] operating in the Astro-WISE environment will reduce each night's data within 8 hours.

In writing the specifications for the detector system, we developed metrics applied to batches of CCDs to obtain the required final science performance on average. This approach is important in keeping costs low because restrictive requirements reduce yield and increase risk and price. A good example of how we approached this is the metric for QE and read noise which is based on S/N ratio for the expected signal level from the sky for VIRUS observations. The metric will be calculated for the average of a batch of detectors, along with a minimum QE threshold as a function of wavelength and a maximum read noise threshold for any CCD. This allows the vendor to balance poorer read noise with increased QE and vice versa and provides greater latitude for accepting CCDs without impacting the performance we care about. The resultant increased yield provides the vendor with greater security of predicting yields and hence provides the best price.

The other key specifications are very low cross-talk between the pair of CCDs in each cryostat, and between cryostats, and very low external noise pickup. Since we are searching for detections which are very few correlated resolution elements, we need to understand the noise characteristics of the data extremely well.

The integrated detector system is being provided by Astronomical Research Cameras, Inc., with the University of Arizona Imaging Technology Laboratory providing thinned backside illuminated CCDs with AR coatings optimized for the VIRUS bandpass, as a subcontract from wafers manufactured by Semiconductor Technology Associates, Inc. Since the CCDs come from custom wafer runs, we elected to increase the imaging area to 2064 by 2064 pixels, allowing more latitude for alignment.

The design of the detector package, flex circuit, and controller have been highly customized to the VIRUS application, since the engineering is spread over a large production run. This allowed us to remove most of the complexity associated with the detector head of the Mitchell Spectrograph[52]. Figure 4 shows the layout for a pair of detectors in a single cryostat. The package, machined from Invar-36, is designed for minimum obstruction and hides in the shadow of the field flattener (FF) lens. The CCDs are flat to within +/-10 μm which is allowed by the tolerance analysis. The package has a custom header board that brings the traces to a single connector on one side of the package. A custom flex circuit with complex geometry connects the two detectors to a single 55-pin hermetic bulkhead connector (Fig. 4). The controller connects directly to this connector, without cables, and its form-factor has been customized to fit between the cylinders of the cryostat cover.

The detector package also mounts the FF lens on four Invar flexure clips that set the separation and alignment of the FF to the detector plane. Metrology of each detector is used to control these dimensions when the clips are glued to the field flattener, with the glue-line acting to take up any misalignment. The alignment jig incorporates a laser to establish the axis of the detector head and allows the field flattener to be aligned using the interference pattern generated by its front and back surfaces. Tests show this scheme has 10 μm sensitivity to tilts and decenter, within the required tolerance. Once the FF lens is installed its optical axis defines the axis of the head and allows alignment within the camera.

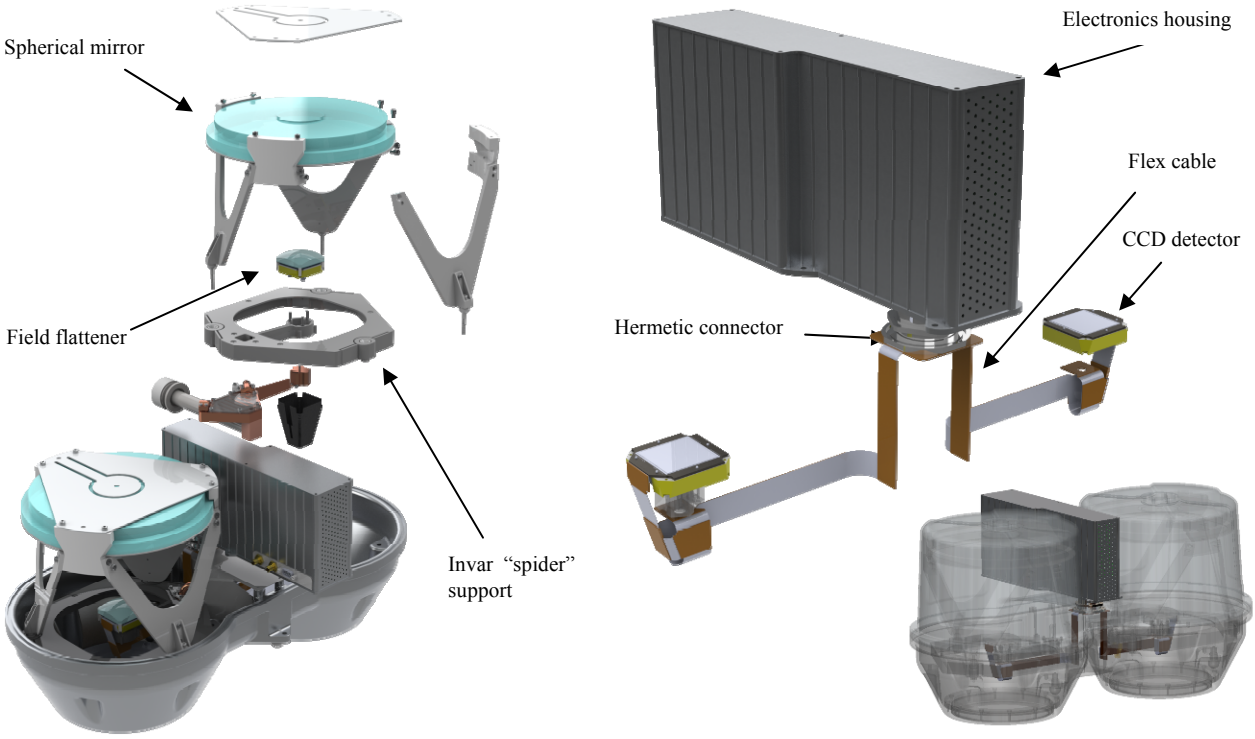

Figure 4. Camera assembly and electronics. Left shows the integration of the two camera channels into the cryostat. Right shows the detector system controller, the flex circuit, and the CCD packages as they integrate into the cryostat.

The detector package with attached FF is then integrated into the "spider" which supports the detector head, cantilevered in the beam. The spider is of post-machined cast Invar-36, and its production is discussed further in Ref. 44. The whole spider is adjusted in all degrees of freedom in an alignment jig to position the FF on the axis of a laser that defines the camera axis. Four lugs are then glued in place to capture the alignment, and they interface to machined features in the cryostat housing. In this way, the alignment of the CCD and FF to the axis of the camera is achieved within the required tolerances of 50 μm in centration and separation, and 0.05 degrees in tilt[41].

Final alignment of the camera is made against a fiducial collimator, grating, and IFU positioning the camera mirror for best focus over the field, using image moment-based wavefront sensing where the mirror is pistoned through focus and the final adjustment to its position then derived from analysis of the set of images[45-46]. This adjustment is done with the detector cold and will utilize a special cryostat back with feed-throughs to make the adjustments and clamp the mirror. The camera mirror is pistoned through focus to record the set of extrafocal images which are analyzed to make the adjustment as deterministic (and hence as quick) as possible. The lab cryogenic system is described in Section 5.1.

The shutter for the system is located in front of the IFU inputs, just below the focal surface in the PFIP[53]. It has a rotary blade design, and a minimum exposure time of 1 second. The shutter is located remotely from the detector controllers and is commanded separately. Exposures are coordinated via the Telescope Control System, which sends simultaneous shutter-open commands to the shutter control system and to the VIRUS Data Acquisition System (VDAS) that controls the detector system. Timing between the shutter and the VDAS is maintained with a Network Time Protocol server, synchronized to GPS time.

Figure 5. Production camera assembly and alignment. Integration of the CCDs and field flattener lenses into the cryostat is shown on the left. Integration of the camera mirror assembly is shown on the right.

The CCD controllers have DC power in and fiber-optic data lines out. To minimize crosstalk, the timing of all CCD clocks is synchronized to a master clock signal distributed over a Low-Voltage Differential Signal (LVDS) system. The data system requires several levels of multiplexing. First, each CCD controller commands two detectors, each with possibly two readout amplifiers. Next, a custom-built 8-way multiplexer combines the output from each set of 8 CCD controllers. Next, the output of each of 12 multplexers is fed into a PCI interface card. Two PCI-to-PCIe expansion chassis are used to connect 6 PCI interface cards each to a PCIe port in the VDAS computer. Finally, the data are transferred via DMA from the PCI interface cards into the VDAS memory. From there, the data are passed to a "QuickLook" pipeline, and also written to disk as separate FITS files, one for each detector, to aid parallel processing of the pixels in an on-site array of CPUs. The QuickLook pipeline includes many of the algorithms developed for the full reduction of the VIRUS dataset[51], but is focused on monitoring detector health and data quality, to inform the observer of problems, and when to terminate observations due to poor conditions.

Lab testing has verified very low cross-talk between CCDs in the same cryostat and further cross-talk tests will soon be performed with two cold cryostats within the first production run of 8 cameras, utilizing the full structure of the detector readout system.

4.4 Integral field unit cables

It is essential to couple VIRUS to the HET with fibers due to the weight and space constraints at the prime focus of the telescope. In addition, the variable effects of the changing pupil illumination of HET during a track are mostly removed by azimuthal scrambling along a fiber, producing much greater stability in the data calibration than is possible with an imaging spectrograph. Fiber IFUs can utilize microlens arrays, providing close to 100% fill-factor[54], or be of the simpler “densepak” type[55]. For VIRUS we have elected to use the densepak type of bare fiber bundle to maximize throughput and minimize cost[56]. The primary advantage of lenslets is in coupling the slower f/ratios of typical foci to the fast ratio required to minimize focal ratio degradation[57-59], and such IFUs are ideal for retro-fitting existing spectrographs. Lenslets do not provide perfect images, however, so if there is flexibility to choose the input f/ratio to the fibers and if the fill-factor can be tolerated, trading it against total area, the bare bundle provides the best efficiency[3]. We use a fill factor of 1/3, with the fibers in a hexagonal close pack, and dither the IFU arrays through three positions to fill the area. Note that if the f/ratio of the microlens case is the same as the f/ratio from the telescope in the bare-fiber case, and the lenslets subtend the same area on the sky as the bare fibers, then the fill-factor of the densepak type array

is exactly offset by the larger area that the bundle covers per exposure. So in the case where maximum areal coverage is required, the bare bundle is the preferred solution[2].

The HET site has a median seeing of 1.0 arcsec FWHM, and we initially adopted 1 arcsec^2 per fiber (200 μm core diameter) on the upgraded HET for maximum sensitivity. Subsequent analysis of the trade-off between areal coverage and sensitivity indicates that larger fibers are preferred for HETDEX to maximize the number of detected LAE galaxies. As a result, 1.5 arcsec (266 μm) diameter is the requirement for the production VIRUS units. The current HET corrector is f/4.65, but the future wide-field corrector will have f/3.65. The optics of VIRUS can accommodate an f/ratio of f/3.32 (within the 125 mm pupil size), allowing some focal ratio degradation and accommodation of alignment errors in the subsystems.

IFU development at the Leibniz Institute for Astrophysics (AIP)[56] and University of Texas at Austin (UT)[58,59] has focused on establishing a design that minimizes FRD, maximizes throughput, and is manufacturable in quantity[58]. Careful and rigorous apportioning of tolerances between the components aims to keep 95% of the transmitted light within the spectrograph pupil. Development of the prototype IFUs explored ways of setting up the required matrix of fibers at the input end. Setting up a matrix of fused silica capillary tubes to set the spacing proved very successful, but time-consuming to set up. The alternative, adopted for production, is to use micro-drilled alloy blocks to locate the fibers at the input. Anti-reflection coated fused silica cover plates are bonded (immersed) to the polished surface of each IFU with index-matching couplant to minimize insertion losses. Measurements of FRD and throughput before and after immersing the ends demonstrate marked improvement for many fibers, and results in very uniform throughput between fibers[56-58]. At the output of the bundle, the fibers are arrayed in a line, immersed against the curved back face of a cylindrical lens, and fanned out with their axes pointing perpendicular to the collimator mirror (and to the lens). This layout allows collimation of the beam to be achieved with only one spherical mirror, leading to a very efficient design. The spacing between fibers is achieved by bonding the fibers to a monolithic groove plate of stainless steel. Figure 6 shows images of the slit and input ends of fiber cables produced during development.

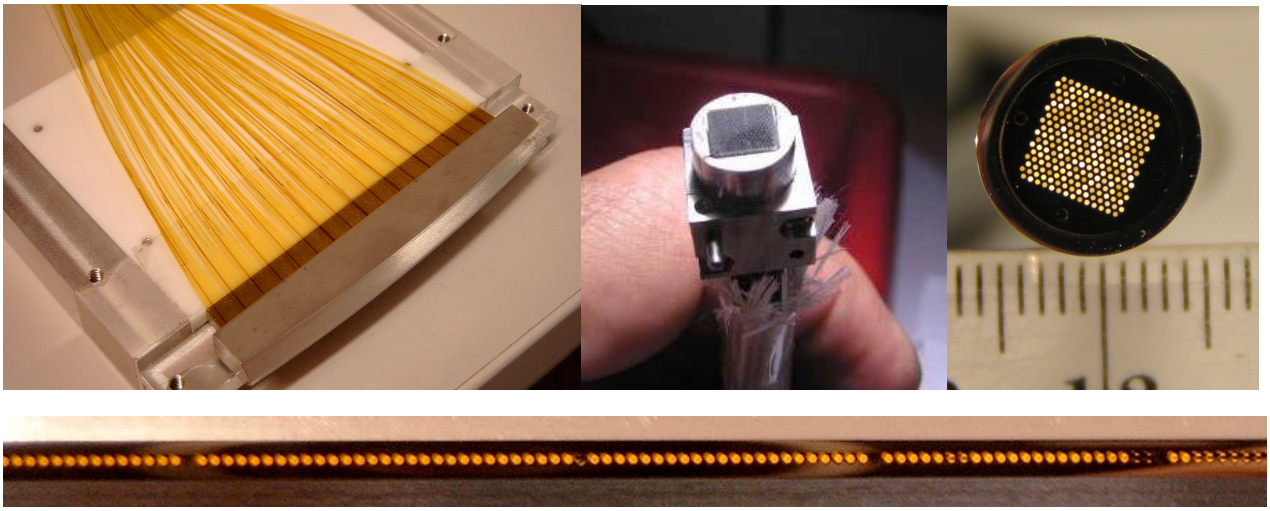

Figure 6: IFU development. Left shows pseudo-slit output of the IFU bundle. The fibers are arrayed on a precision grooved plate that sets the spacing and angle between fibers. The fibers are arrayed perpendicular to the back surface of a cylindrical lens bonded to the convex surface of the plate. Middle and Right show input heads with the matrix set by fused silica capillaries and drilled block, respectively. Bottom shows a section of the output slit.

The production fiber cables each contain 448 fibers with 266 μm cores, and we have kept the design as simple and lightweight as possible (Fig 7). The input head consists of a precision micro-drilled block into which the fibers are fed which is in turn clamped within a stainless steel shell that provides the mounting features. The fibers are glued in with epoxy and then cut off and polished. At the exit, the cable bifurcates within a slit housing into two slits with the fibers glued to grooved blocks of the same design as for the Mitchell Spectrograph. Input and output are bonded to a thin fused silica lens and a cylindrical lens, respectively, both AR coated.

The physical design of the cables has benefitted greatly from the use of prototype bundles on the Mitchell Spectrograph, which has been taking data for 5 years. We uncovered an interesting behavior when fibers in the corners of the square input array started to show variable and lower throughput on the sky. This was traced to the way the cable was being handled. This cable was 15 m long to allow the Mitchell Spectrograph to be deployed on the HET and each month it was coiled and uncoiled during the mounting process. Twists introduced into the cable resulted in a torsional force at the head, which affected the fibers in the corners, preferentially. This was verified with tests in the lab which revealed significant stress-induced FRD for these fibers. Shaking out the cable relieved the stress and we now dress the cable in a large loop rather than coiling it up. Interestingly the effect did not show itself until after more than a year of use, so it is possible that the constant handling of the cable caused these fibers to become more sensitive to the torsional stress. In this respect the long track-record of the Mitchell Spectrograph has proven valuable in evaluating the design.

Figure 7. Production IFU cables at AIP. Left and middle images show the slit assembly with the two slit blocks that feed the pair of spectrographs within a VIRUS unit. The slit assembly mounts to the collimator kinematically. The cable length is 22 m. Right shows nine IFUs input heads mounted as they will be at the HET focus. Three screws and a pin locate the heads. AR coated cover plates are not yet applied in this view. The heads have a ¼ fill-factor in the field of view. This configuration provides the ability to fill in the field of view by offsetting the telescope to four positions.

The conduit housing the fiber cables has undergone an extensive design evaluation and prototyping. It is important that the fiber not piston significantly in and out of the conduit where it exits the cable into the slit box. Such pistoning might occur with changes in axial load or ambient temperature swings, and we are particularly concerned about shipping and handling during installation. We also wish to minimize the weight of the conduit which can dominate the total weight, and have adopted a custom fully interlocked aluminum conduit with PVC sheathing supplied by Hagitec. The ID is 13 mm. As with our previous cables we have an inner sock of Kevlar to protect the fiber from the internal structure of the conduit. In order to stabilize the length of the conduit we tension this inner sock at assembly so that the conduit is somewhat compressed and the resultant spring constant is high. The Kevlar sock has a minimum diameter chosen so as not to constrict the fiber, but still fit in the ID of the conduit. The Kevlar is tensioned during assembly, which stabilizes the length of the conduit assembly and prevents fibers “pumping” in and out and developing torsional stress. We have taken this design through the full range of motions expected at HET (and more) and not seen any sign of the fiber pistoning in and out of the conduit at its exit.

The exit focal ratio from the cable and the position of the pupil from each fiber at the instrument pupil depend on more than FRD. Tilts of the fibers (individually and as a group) at the input make the exit focal ratio faster, and tilts at the slit cause the pupil to translate in the instrument. The VIRUS optical design allows for 10 mm extra pupil diameter, and all these effects have been toleranced and added to the FRD, so that in total at least 95% of the light passes unvignetted through the instrument pupil.

In production, we provide the manufacturers with kits of parts (fiber, mechanical parts, conduit, etc.) and they do the assembly and polishing of the ends. Final integration of the slit blocks into the output slit assembly is done at AIP. We have established three production lines, based on qualification work at several vendors. Each is capable of producing at least one IFU per month. Acceptance test and evaluation facilities have been set up at AIP. These include microscope examination of polish of the input and output ends against fiducial standards, FRD testing, throughput testing, and fiber mapping and position measurement. A final system test will be performed on each cable with a fiducial spectrograph, generating a report and metadata that will be used by the reduction software and in record keeping.

4.5 IFU Lifetime Test

While five years of use on the Mitchell Spectrograph has provided information on the durability of IFU cables, we wanted to conduct a more controlled test in order to uncover any design issues related to durability in the production IFUs before committing to full production. In particular, we first wanted to understand how the fibers behave while in motion, and that might depends on the rate of fiber motion. Second, we wished to monitor how the properties of a VIRUS fiber bundle change due to the accumulation of wear. In order to explore these questions we simulated 10.2 years of wear (188.7 km of linear travel) on a single fiber bundle. The simulated motion was carried out between February and May, 2011 on test rig designed and built for this purpose[60]. Results of the lifetime test are described in Ref. 59, and have qualified the cable design for final manufacture.

4.6 Sofware Development

One place where the parallelized nature of VIRUS is a huge advantage is in data reduction software development. Many instruments have suffered from the late arrival of reduction software or from unexpected instrumental features that require the development of new software methods to account for them. Since the VIRUS units will be very close to identical, and very similar to the Mitchell Spectrograph, we have had the advantage of having a full test-bed for the software in operation for several years.

The software for VIRUS must process a highly parallel data stream, quickly, and detect single-line objects, reliably. Development of the final software pipeline for reduction of VIRUS data is being led by MPE. Since VIRUS is naturally a parallel instrument, all the requirements for and attributes of the software have been developed and tested on the prototype. This was a key motivation for the deployment of the Mitchell Spectrograph on the telescope early in the project. Two pipelines have been developed, one in Texas called VACCINE[47] and the other in Munich, called CURE[51]. VACCINE has been used primarily to reduce and analyze data from the pilot survey on the McDonald 2.7 m, while the algorithms of CURE are tuned for use on the HET. The difference is driven primarily by the plate scale difference between the telescopes. On the 2.7 m, the fibers are significantly larger than the image size, while on HET they are comparable. This leads to differences in the detection algorithm, but not the data reduction methods. Care is being taken to propagate errors and avoid interpolation through resampling of data, which leads to position-dependent smoothing and can alter the noise characteristics. CURE uses a Bayesian detection algorithm that assigns a likelihood of a source to every (spatial and spectral) resolution element. Tests show robust rejection of cosmic rays and reliable detection of 5-σ line flux objects, as required for HETDEX. The stability requirements for the instrument (Sec. 2) are driven by the need to know the statistical weight of each pixel, particularly in the spatial dimension, across the fiber profiles, where small movement of the image on the detector can change the weights greatly. We have also demonstrated sky subtraction to the Poisson noise limit, with both pipelines, aided by the fact that most of the fibers of VIRUS are observing sky in any exposure.

We have exploited the advantage to having the ability to exercise software on real data this early in the project, and we expect to come on line with a fully operational and debugged pipeline when VIRUS is turned on, not least because early production VIRUS units will be used on sky prior to deployment of the full instrument. This is a key advantage of a highly replicated instrument, particularly since such instruments by definition generate large volumes of data.

5. DEPLOYMENT ON HET (CRYOGENIC SYSTEM AND SUPPORT STRUCTURE)

The distributed layout of the VIRUS array presents a significant challenge for the cryogenic design[50,61]. Allowing 5 W heat load for each detector, with all losses accounted for and a 50% margin, the cooling source is required to deliver 3,600W of cooling power. We engaged George Mulholand of Applied Cryogenics Technology to evaluate the options and provide an initial design. Following a trade off between cryocoolers, small pulse-tubes and liquid nitrogen based systems, it is clear that from a reliability and cost point of view liquid nitrogen is the best choice[61]. The problem of distributing the coolant to the distributed suite of spectrographs is overcome with a gravity siphon system fed by a large external dewar. A trade-off between in-situ generation of the LN_2 in an on-site liquefaction plant, and delivery by tanker has been made, with the result that the delivery option is both cheaper and more reliable. The 11,000 gallon holding dewar would have in excess of 4 weeks operation capacity, and would be refilled every 2 weeks. The cryogenic system is illustrated in Fig. 8.

An important aspect of the cryogenic design is the requirement to be able to remove a camera cryostat from the system for service, without impacting the other units. This is particularly difficult in a liquid distribution system. A

design has been developed that combines a standard flexible stainless steel vacuum jacketed line (SuperFlex) to a cryogenic bayonet incorporating copper thermal connector contacts into each side of the bayonet. When the bayonet halves are brought together they close the thermal contact. The resulting system is completely closed, i.e., it is externally dry with no liquid nitrogen exposure. The camera end of the connector is connected by a copper cold finger to the detector. This design has another desirable feature: in normal operation the SuperFlex tube slopes downwards and the bayonet is oriented vertically. Liquid evaporation will flow monotonically up in order to avoid a vapor lock. If the bayonet is unscrewed and raised upwards, a vapor lock will occur and the bayonet will be cut off from the cooling capacity of the liquid nitrogen. This effectively acts as a "gravity switch", which passively turns off cooling to that camera position.

We have made extensive tests on prototypes, applying heat loads to the bayonet, which have performed very well[50]. The temperature rise across the connection is $\Delta T \sim 1.8$ K/Watt of load at 80 K. Modeling of the full thermal path has been undertaken, under the requirement of having the CCD temperature at -140 C, with no heater power. The performance of the bayonet is significantly better than the requirement, and represents less than 20 K temperature rise across the connection for the expected load. We will run the CCDs at about -110 C, controlled via heating resistors and a control loop based on an RTD sensor. The performance of the bayonet is not changed when the connection is broken and remade.

We have been running a lab cryogenic system for VIRUS testing for the past 2 years. It is a microcosm of the final VCS having a large external dewar, a header tank with "keep full" auto-fill system, and a single flex line and bayonet. The system is extremely reliable, and has been used to demonstrate that the VIRUS cryostats will hold vacuum, when

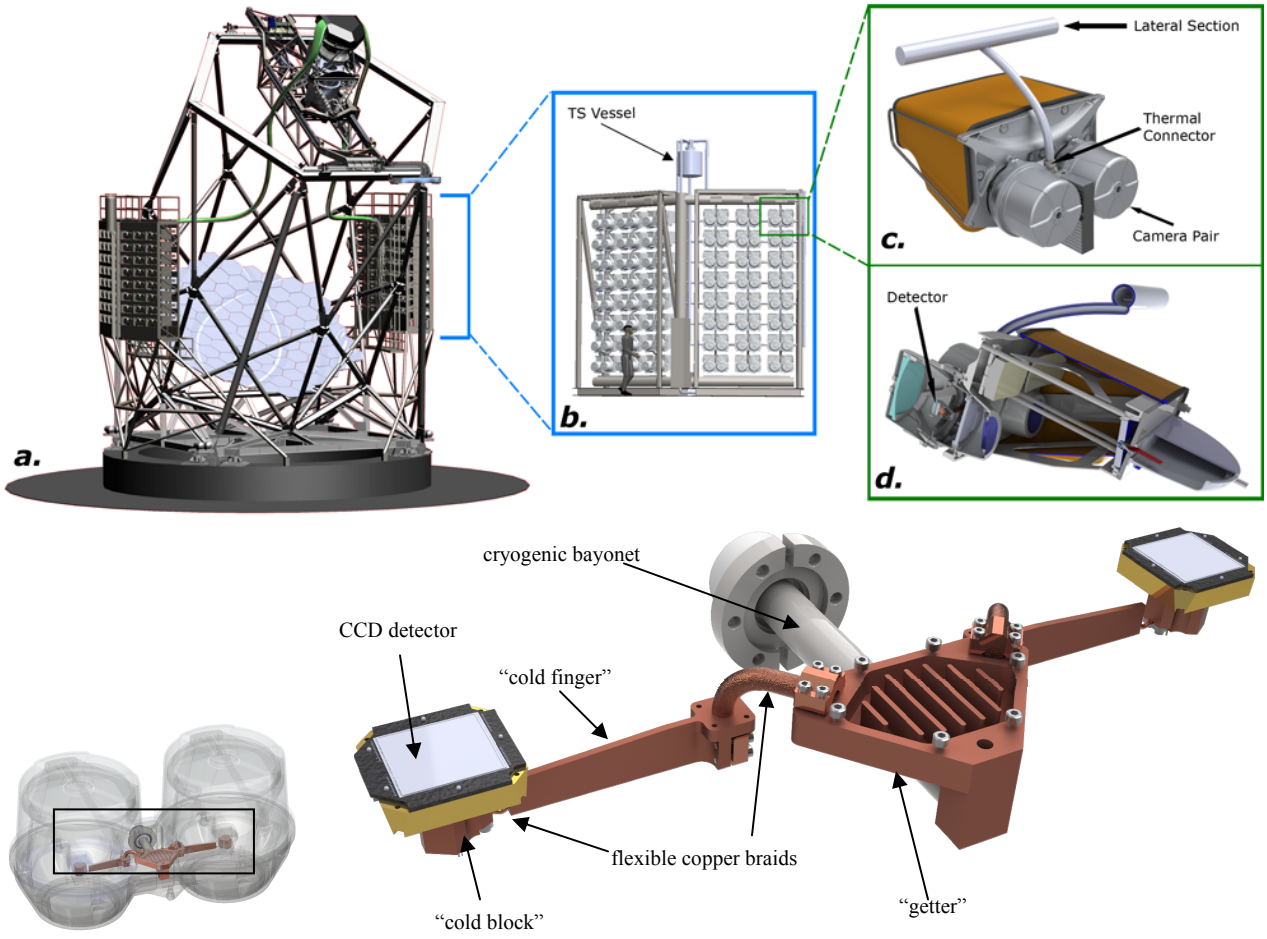

Figure 8. Camera cryogenic system. Top panels show the liquid nitrogen distribution system on the telescope and thermal connector to the cryostat. An external dewar keeps the two thermal siphon (TS) vessels filled, which feed the manifolds. The lower panels show the cold link interior to the cryostat which cools two detectors via cold links from the bayonet.

kept cold, for at least 4 months without external intervention such as use of an ion pump. This performance allows us to avoid the cost of adding ion pumps and vacuum gauges to each camera, and instead rely on a maintenance regimen at HET that regularly warms, vacuum pumps, and then re-cools the cryostats in-situ, every 3-4 months. Based on the extensive prototype testing we are confident that the full cryogenic system will be robust. The contract for the fabrication is about to be awarded.

The VIRUS support structure (VSS[63]), shown in Fig. 1, supports and houses the spectrograph units and rotates on air bearings with the telescope structure when the azimuth is changed. The four enclosures can each house up to 24 VIRUS units. They have access panels for each unit to allow servicing of an individual unit, and circulate filtered, conditioned air that is controlled in temperature to track the ambient temperature sufficiently well that the surface of the enclosures is within 0.5 C of ambient. The VCS manifolds interface to the VSS which consists of the enclosures for VIRUS and support structure that holds them stiffly but without interacting with the main telescope frame during observation. When azimuth is changed, the VSS picks up on air bearings as does the main structure and is dragged round to position by the main azimuth drive and then set in place.

7. THE VIRUS FUTURE

VIRUS was designed from the outset to allow exchange of gratings to change wavelength ranges and resolutions, and the Mitchell Spectrograph is used on the McDonald 2.7 m Smith Telescope with four different VPH gratings. Due to the large size of the fibers projected on the sky, it is very sensitive for low surface brightness extended features, for which the sensitivity surpasses that of instruments on the largest telescopes. In addition to this flexibility and sensitivity, the generic nature and massively replicable characteristic of the instrument can allow us to adapt the instrument to a wide range of not only telescope diameters (1m ~ 40m), but also observing modes (single to multiple objects), in a very cost-effective manner. On small telescopes, the IFU can cover very large fields of view with large spatial elements ideal for studying resolved galaxies, while on large telescopes the same IFU can observe single objects in varying image quality, while obtaining a simultaneous background observation. VIRUS allows many different slicing modes between field and wavelength coverage/resolution, and a few of them are illustrated in the following examples.

The current HET Low-Resolution Spectrograph[63] is incompatible with the WFU and will be replaced with a more capable broad-band fiber-fed instrument based on VIRUS, called LRS2[64,65]. It takes advantage of the fact that VIRUS was designed to be easily adapted to a wide range of spectral resolutions, and wavelength ranges by changing dispersers and optics coatings. LRS2 is fed by a 7x12 arcsec^2 lenslet coupled fiber IFU, covers 350-1100 nm, simultaneously at a fixed resolving power R~1800, with the wavelength range split with dichroics into four channels shared between two VIRUS units, one for the blue and red wavelength range (350 - 630 nm) and the other for the red and far-red range (630-1100 nm). It uses the multiplex power of VIRUS to cover wavelength, rather than wide area. Only minimal modification from the base VIRUS design in gratings (for both units) and in the detectors (to fully depleted thick CCDs for the far-red unit only) is required. We expect to deploy the blue unit when we install VIRUS. LRS2 is a powerful instrument serving the HET strengths in survey follow-up, synoptic observations, and transient events. It will be particularly useful for following up emission-line objects detected with VIRUS at higher resolution, and can be used in parallel with VIRUS.

The other immediate evolution of the VIRUS design has been the instrument VIRUS-W, destined for the new Munich Wendelstein Observatory[66]. The instrument is targeted at studies of resolved galaxies, specifically spiral galaxy bulges, a proven strength of the Mitchell Spectrograph. It uses many of the design elements of VIRUS, but aims for higher resolution over a more restricted bandpass. The camera is refractive and two VPHG grisms can be exchanged to observe 475 - 560 nm at R~2300 or 493 - 544 nm at R~6500. The IFU has 267 fibers, each 4.24 arcsec diameter covering a field of 144 x 75 arcsec^2.

8. SUMMARY AND STATUS

HETDEX, consisting of the WFU, VIRUS, and the blind spectroscopic survey of 420 sq. degrees is fully funded and completion of the WFU and VIRUS is projected for early 2014. The production of VIRUS has started (Fig. 9 shows the First Article production unit) and is projected to span the next 12 months. 20 units (IFU, camera, and collimator) should be complete this calendar year.

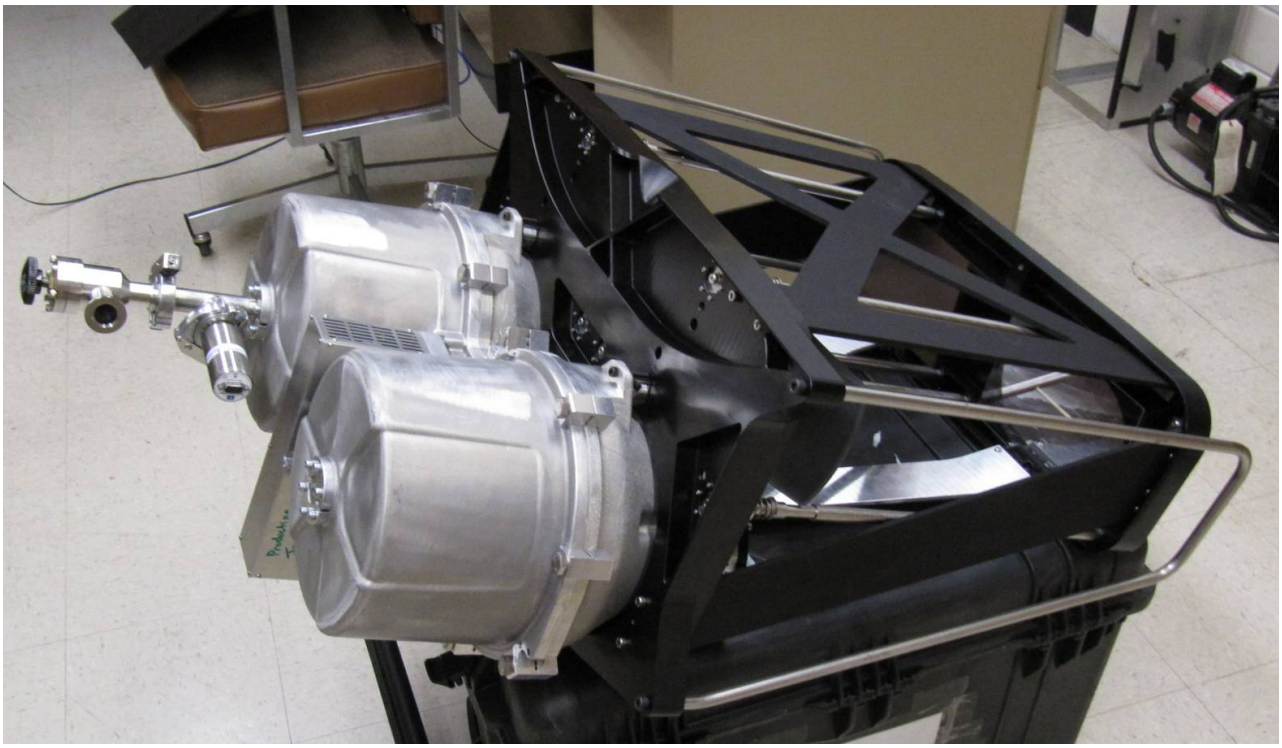

Figure 9. VIRUS First Article Production Spectrograph Unit with cover removed. This unit has proven all the production parts and is within specifications for image quality and other requirements.

ACKNOWLEDGEMENTS

HETDEX is run by the University of Texas at Austin McDonald Observatory and Department of Astronomy with participation from the Ludwig-Maximilians-Universität München, Max-Planck-Institut für Extraterrestriche-Physik (MPE), Leibniz-Institut für Astrophysik Potsdam (AIP), Texas A&M University, Pennsylvania State University, Institut für Astrophysik Göttingen, University of Oxford and Max-Planck-Institut für Astrophysik (MPA). In addition to Institutional support, HETDEX is funded by the National Science Foundation (grant AST-0926815), the State of Texas, the US Air Force (AFRL FA9451-04-2-0355), by the Texas Norman Hackerman Advanced Research Program under grants 003658-0005-2006 and 003658-0295-2007, and by generous support from private individuals and foundations.

Financial support for innoFSPEC Potsdam of the German BMBF program *Unternehmen Region* (grant no. 03Z2AN11), and of Land Brandenburg, MWFK, is gratefully acknowledged. MMR also acknowledges support by the the German BMI program *Wirtschaft trifft Wissenschaft*, grant no. 03WWBB105.

We thank the staffs of McDonald Observatory, AIP, MPE, Oxford University Department of Physics, and the University of Texas Center for Electromechanics, for their contributions to the development of the WFU and VIRUS.

REFERENCES

1. e.g. M. Ouchi, M., et al., "Large-Scale Filamentary Structure around the Protocluster at Redshift z = 3.1," ApJ, **634**, 125 (2005); Gronwall, et al., "Lyα Emission-Line Galaxies at z = 3.1 in the Extended Chandra Deep Field-South," ApJ, **667**, 79 (2007); L. Guaita, et al., "Ly-α Emitting Galaxies at z = 2.1 in ECDF-S: Building Blocks of Typical Present-day Galaxies?" ApJ, **714**, 255 (2009);
2. e.g. C. Martin et al., "A Magellan IMACS Spectroscopic Search for Lyα-emitting Galaxies at Redshift 5.7," ApJ, **679**, 942 (2008); M. Rauch et al., "A Population of Faint Extended Line Emitters and the Host Galaxies of Optically Thick QSO Absorption Systems," ApJ, **681**, 586, (2008)

3. G.J. Hill, P.J. MacQueen, P. Palunas, A. Kelz, M.M. Roth, K. Gebhardt, & F. Grupp, "VIRUS: a hugely replicated integral field spectrograph for HETDEX", *New Astronomy Reviews*, **50**, 378 (2006); G.J. Hill, P.J. MacQueen, J.R. Tufts, A. Kelz, M.M. Roth, W. Altmann, P. Segura, M. Smith, K. Gebhardt, & P. Palunas, "VIRUS: a massively-replicated IFU spectrograph for HET," *Proc. SPIE*, **6269**-93 (2006)
4. G.J. Hill, P.J. MacQueen, M.P. Smith, J.R. Tufts, M.M. Roth, A. Kelz, J. J. Adams, N. Drory, S.I. Barnes, G.A. Blanc, J.D. Murphy, K. Gebhardt, W. Altmann, G.L. Wesley, P.R. Segura, J.M. Good, J.A. Booth, S.-M. Bauer, J.A. Goertz, R.D. Edmonston, C.P. Wilkinson, "Design, construction, and performance of VIRUS-P: the prototype of a highly replicated integral-field spectrograph for HET", *Proc. SPIE*, **7014**-257 (2008)
5. G.J. Hill, et al., "VIRUS: a massively replicated 33k fiber integral field spectrograph for the upgraded Hobby-Eberly Telescope," *Proc. SPIE*, **7735**-21 (2010)
6. R.D. Savage, J.A. Booth, K. Gebhardt, J.M. Good, G.J. Hill, P.J. MacQueen, M.D. Rafal, M.P. Smith, B.L. Vattiat, "Current Status of the Hobby-Eberly Telescope Wide Field Upgrade and VIRUS", *Proc. SPIE*, **7012**-10 (2008)
7. R. Savage, et al., "Current Status of the Hobby-Eberly Telescope wide field upgrade," *Proc. SPIE*, **7733**-149 (2010)
8. G.J. Hill, *et al*., "Current status of the Hobby-Eberly Telescope wide field upgrade," *Proc. SPIE*, **8444**-19 (2012)
9. R.M. Bacon "The second-generation VLT instrument MUSE ", Proc. SPIE, **7735**-7 (2010)
10. See papers cited at www.hetdex.org
11. Hill, G.J., Gebhardt, K., Komatsu, E., Drory, N., MacQueen, P.J., Adams, J.A., Blanc, G.A., Koehler, R., Rafal, Roth, M.M., Kelz, A., Grupp, F., Murphy, J., Palunas, P., Gronwall, C., Ciardullo, R., Bender, R., Hopp, U., and Schneider, D.P., 2008, "The Hobby-Eberly Telescope Dark Energy Experiment (HETDEX): Description and Early Pilot Survey Results", in Panoramic Views of the Universe, ASP Conf. Series, vol **399**, p 115 (arXiv:0806.0183v1)
12. J.A. Booth, M.J. Wolf, J.R. Fowler, M.T. Adams, J.M. Good, P.W. Kelton, E.S. Barker, P. Palunas, F.N. Bash, L.W. Ramsey, G.J. Hill, P.J. MacQueen, M.E. Cornell, & E.L. Robinson, "The Hobby-Eberly Telescope Completion Project", in *Large Ground-Based Telescopes*, Proc SPIE **4837**, 919 (2003)
13. J.A. Booth, P.J. MacQueen, J.G. Good, G.L. Wesley, P.R. Segura, P. Palunas, G.J. Hill, R.E. Calder, "The Wide Field Upgrade for the Hobby-Eberly Telescope", Proc. SPIE, **6267**-97 (2006)
14. G.J. Hill, P.J. MacQueen, M.D. Shetrone, & J.A. Booth, "Present and future instrumentation for the Hobby-Eberly Telescope", Proc. SPIE, **6269**-5 (2006)
15. G.J. Hill, P.J. MacQueen, P. Palunas, S.I. Barnes, M.D. Shetrone "Present and future instrumentation for the Hobby-Eberly Telescope", Proc. SPIE, **7014**-5 (2008)
16. D.A.H. Buckley, G.P. Swart, J.G. Meiring, "Completion of the Southern African Large Telescope", *Proc. SPIE*, **6267**-19 (2006)
17. J. H. Burge, S. D. Benjamin, M. B. Dubin, S. M. Manuel, M. J. Novak, Chang Jin Oh, M. J. Valente, C. Zhao, J. A. Booth, J. M. Good, G. J. Hill, H. Lee, P. J. MacQueen, M. D. Rafal, R. D. Savage, M. P. Smith, B. L. Vattiat, "Development of a wide-field spherical aberration corrector for the Hobby Eberly Telescope", Proc. SPIE, **7733**-51 (2010)
18. J. Good, et al., "Design of performance verification testing for HET wide-field upgrade tracker in the laboratory," Proc. SPIE, **7739**-152 (2010)
19. M.S. Worthington, et al., "Design and analysis of the Hobby-Eberly Telescope Wide Field Upgrade bridge," Proc. SPIE, **7733**-147 (2010)
20. N.T. Mollison, et al., "Design and development of a long-travel positioning actuator and tandem constant force actuator safety system for the Hobby-Eberly Telescope wide field upgrade," Proc. SPIE, **7733**-150 (2010)
21. G.A. Wedeking, et al., "Kinematic optimization of upgrade to the Hobby-Eberly Telescope through novel use of commercially available three-dimensional CAD package," Proc. SPIE, **7733**-148 (2010)
22. J.J. Zierer, Jr., G.A. Wedeking, J.H. Beno, J.M. Good, "Design, testing, and installation of a high-precision hexapod for the Hobby-Eberly Telescope dark energy experiment (HETDEX)," Proc. SPIE, **8444**-176 (2012)
23. J.R. Mock, et al., "Tracker controls development and control architecture for the Hobby-Eberly Telescope Wide Field Upgrade," Proc. SPIE, **7733**-152 (2010)
24. R.J. Hayes, et al., "Use of failure modes and effects analysis in design of the tracker system for the HET wide-field upgrade," Proc. SPIE, **8449**-56 (2012)
25. M.S. Worthington, et al., "Design and development of a high-precision, high-payload telescope dual-drive system," Proc. SPIE, **7733**-201 (2010)
26. N.T. Mollison, et al., "Collaborative engineering and design management for the Hobby-Eberly Telescope wide field upgrade," Proc. SPIE, **7738**-84 (2010)

27. J.H. Beno, *et al*., "HETDEX tracker control system design and implementation," Proc. SPIE, **8444**-211 (2012)
28. H. Lee, et al., "Analysis of active alignment control of the Hobby-Eberly Telescope wide field corrector using Shack-Hartmann wavefront sensors," Proc. SPIE, **7738**-18 (2010)
29. H. Lee, et al., "Metrology systems for the active alignment control of the Hobby-Eberly Telescope wide-field upgrade," Proc. SPIE, **7739**-28 (2010)
30. H. Lee, et al., "Orthonormal aberration polynominals over arbitrarily obscured pupil geometries for wavefront sensing in the Hobby-Eberly Telescope," Proc. SPIE, **7738**-59 (2010)
31. H. Lee, et al., "Metrology systems of Hobby-Eberly Telescope wide field upgrade," Proc. SPIE, **8444**-181 (2012)
32. H. Lee, et al., "Surface figure measurement of the Hobby-Eberly Telescope primary mirror segments via phase retrieval and its implications for the wavefront sensing in the new wide-field upgrade," Proc. SPIE, **7738**-58 (2010)
33. J.J. Adams, J. Uson, G.J. Hill, & P.J. MacQueen, "A new z = 0 metagalactic UV background limit," ApJ, **728**, 107 (2011)
34. J.J. Adams, G.J. Hill, & P.J. MacQueen, "B20902+34: a collapsing proto-giant elliptical galaxy at z=3.4", ApJ, **694**, 314 (2009)
35. G.A. Blanc, A. Heiderman, K. Gebhardt, N.J. Evans, J. Adams, "The Spatially Resolved Star Formation Law From Integral Field Spectroscopy: VIRUS-P Observations of NGC 5194", ApJ, **704**, 842 (2009); G.A. Blanc, et al., "The VIRUS-P Exploration of Nearby Galaxies (VENGA): Survey Design and First Results", in *Third Biennial Frank N. Bash Symposium, New Horizons in Astronomy*, ASP Conf. Ser., in press (2010) (2010arXiv1001.5035B)
36. P. Yoachim et al.,, ApJ, 716, L4-8 (2010).
37. J.J. Adams, et al., "The Central Dark Matter Distribution of NGC 2976", ApJ, **745**, 92 (2012)
38. J.J. Adams, et al., "The HETDEX Pilot Survey I. Survey Design, Performance, and Catalog of Emission-Line Galaxies," ApJS, **192**, 5 (2011)
39. G.A. Blanc, et al., "The HETDEX Pilot Survey II: The Evolution of the Ly-α Escape Fraction from the UV Slope and Luminosity Function of 1.9<z<3.8 LAEs," ApJ, **736**, 31 (2011)
40. S.L. Finkelstein, S.L., et al., "The HETDEX Pilot Survey III: The Low Metallicities of High-Redshift Lyman Alpha Galaxies," ApJ, 729, 140 (2011)
41. H. Lee, et al., "VIRUS optical tolerance and production," Proc. SPIE, **7735**-140 (2010)
42. B. Vattiat, et al., "Mechanical design evolution of the VIRUS instrument for volume production and deployment," Proc. SPIE, **7735**-264 (2010)
43. T. Prochaska, et al., "VIRUS spectrograph assembly and alignment procedures," *Proc. SPIE*, **8446**-193 (2012)
44. S.E. Tuttle, et al., "Initial results from VIRUS production spectrographs," *Proc. SPIE*, **8446**-221 (2012)
45. H. Lee, G.J. Hill, "Image moment-based wavefront sensing for in-situ full-field image quality assessment," Proc. SPIE, **8450**-191 (2012)
46. H. Lee, G.J. Hill, S.E. Tuttle, B.L. Vattiat, "Fine optical alignment correction of astronomical spectrographs via in-situ full-field moment-based wavefront sensing," Proc. SPIE, **8450**-192 (2012)
47. J.J. Adams, G.J. Hill, and P.J. MacQueen, "Volume Phase Holographic Grating Performance on the VIRUS-P Instrument", *Proc. SPIE*, **7014**-258 (2008)
48. T.S. Chonis, G.J. Hill, J.C. Clemens, B. Dunlap, H. Lee, "Methods for evaluating the performance of volume phase holographic gratings for the VIRUS spectrograph array ," Proc. SPIE, **8446**-209 (2012)
49. E.B. Burgh, M.A. Bershady, K.B. Westfall, and K.H. Nordsieck, "Recombination Ghosts in Littrow Configuration: Implications for Spectrographs Using Volume Phase Holographic Gratings," PASP **119**, 1069 (2007)
50. T.S. Chonis, et al., "Development of a cryogenic system for the VIRUS array of 150 spectrographs for the Hobby-Eberly Telescope," Proc. SPIE, **7735**-265 (2010)
51. J. M. Snigula, et al., "Cure-WISE: HETDEX data reduction with Astro-WISE," Proc. SPIE, **8451**-78 (2012)
52. J.R. Tufts, P.J. McQueen, M.P. Smith, P.R. Segura, G.J. Hill, R.D. Edmonston, "VIRUS-P: camera design and performance", *Proc. SPIE*, **7021**-10 (2008)
53. B.L. Vattiat, et al., "Design, testing, and performance of the Hobby Eberly Telescope prime focus instrument package," Proc. SPIE, **8446**-269 (2012)
54. e.g. J.R. Allington-Smith *et. al*., "Integral Field Spectroscopy with the Gemini Multiobject Spectrograph. I. Design, Construction, and Testing", PASP, **114**, 892 (2002)
55. S.C. Barden & M.A. Wade, "DensePak and spectral imaging with fiber optics", in *Fiber optics in astronomy*; Proceedings of the Conference, Tucson, AZ, Apr. 11-14, 1988 (A90-20901 07-35). San Francisco, CA, Astronomical Society of the Pacific, 1988, p. 113-124

56. A. Kelz, S.M. Bauer, F. Grupp, G.J. Hill, E. Popow, P. Palunas, M.M. Roth, P.J. MacQueen, U. Tripphahn, "Prototype development of the integral-field unit for VIRUS", *Proc. SPIE*, **6273**, 121 (2006)
57. e.g. J. Schmoll, M.M. Roth, & U. Laux, "Statistical Test of Optical Fibers for Use in PMAS, the Potsdam Multi-Aperture Spectrophotometer," PASP, **115**, 854 (2003)
58. J.D. Murphy, P. Palunas, F. Grupp, P.J. McQueen, G.J. Hill, A. Kelz, M.M. Roth, "Focal ratio degradation and transmission in VIRUS-P optical fibers", *Proc. SPIE*, **7018**-104 (2008)
59. J.D. Murphy, et al., "The Effects of Motion and Stress on Optical Fibers", Proc. SPIE, **8446**-207 (2012)
60. I. Soukup, et al., "Design of the fiber optic support system and fiber bundle accelerated life test for VIRUS," Proc. SPIE, **7735**-180 (2010)
61. M.P. Smith, G.T. Mulholland, J.A. Booth, J.M. Good, G.J. Hill, P.J. MacQueen, M.D. Rafal, R.D. Savage, B.L. Vattiat, "The cryogenic system for the VIRUS array of spectrographs on the Hobby Eberly Telescope", *Proc. SPIE*, **7018**-117 (2008)
62. J.T. Heisler, et al., "Integration of VIRUS spectrographs for the HET dark energy experiment," Proc. SPIE, **7733**-153 (2010)
63. Hill, G. J., Nicklas, H., MacQueen, P. J., Tejada de V., C., Cobos D., F. J., and Mitsch, W., "The Hobby-Eberly Telescope Low Resolution Spectrograph", in *Optical Astronomical Instrumentation*, S. D'Odorico, Ed., Proc. SPIE, **3355**, 375 (1998)
64. H. Lee, et al., "LRS2: a new low-resolution spectrograph for the Hobby-Eberly Telescope and its application to scalable spectrographs for the future of extremely large telescopes," Proc. SPIE, **7735**-276 (2010)
65. T.S. Chonis, H. Lee, G.J. Hill, M.E. Cornell, S.E. Tuttle, B.L. Vattiat, "Design and construction progress of LRS2-B: a new low resolution integral-field spectrograph for the Hobby-Eberly Telescope," Proc. SPIE, **8446**-103 (2012)
66. M.H. Fabricius, S. Barnes, R. Bender, N. Drory, F. Grupp, G.J Hill, U. Hopp, P.J. MacQueen, "VIRUS-W: an integral field unit spectrograph dedicated to the study of spiral galaxy bulges", *Proc. SPIE*, **7014**, 234 (2008)